

Analysis of directional emission in square resonator lasers with an output waveguide

Wei Zhao (赵伟) and Yongzhen Huang (黄永箴)

State Key Laboratory on Integrated Optoelectronics, Institute of Semiconductors,
Chinese Academy of Sciences, Beijing 100083

Received December 8, 2006

Square microcavity laser with an output waveguide is proposed and analyzed by the finite-difference time-domain (FDTD) technique. For a square resonator with refractive index of 3.2, side length of $4\ \mu\text{m}$, and output waveguide of $0.4\text{-}\mu\text{m}$ width, we have got the quality factors (Q factors) of 6.7×10^2 and 7.3×10^3 for the fundamental and first-order transverse magnetic (TM) mode near the wavelength of $1.5\ \mu\text{m}$, respectively. The simulated intensity distribution for the first-order TM mode shows that the coupling efficiency in the waveguide reaches 53%. The numerical simulation shows that the first-order transverse modes have fairly high Q factor and high coupling efficiency to the output waveguide. Therefore the square resonator with an output waveguide is a promising candidate to realize single-mode directional emission microcavity lasers.

OCIS codes: 140.4780, 140.3410, 140.3570, 230.3990.

Microcavity lasers have attracted a great deal of interest over the past decade because of their potential application in photonic-integrated circuits. The microdisk lasers based on whispering-gallery (WG) modes exhibit very high quality (Q) resonance and low threshold due to the total internal reflection^[1]. However, as a serious disadvantage, the microdisk lasers lack directional emission and high output power because of the circular symmetry and high reflectivity sidewalls. In order to overcome the deficiency, various approaches were pursued such as patterned asymmetries in the microdisk resonators^[2] and the asymmetric resonant cavities with ellipse^[3,4], quadrupolar^[3,5,6], spiral^[7], and stadium-shaped^[8] microdisks. In addition, highly directional coupling outputs were achieved by coupling the microdisk with output waveguide through evanescent fields^[9–12]. Recently, the polygonal resonant cavities, such as triangular^[13] and square-shaped^[14,15] cavities, have received a great deal of attention due to their lower symmetries. We have investigated the mode characteristics of equilateral-triangle-resonator (ETR) experimentally^[16] and realized the room temperature continuous-wave (CW) electrically injected lasing operation for the ETR lasers directly coupling with an output waveguide^[17].

The theoretical analysis and experimental results indicate that square resonator is a good candidate for realizing single-mode microcavity lasers^[14,15]. The quasi-WG modes with odd parities relative to the square diagonal have much higher Q factors than the corresponding even modes. However, the directional emission for square resonators is still a problem, which is important for practical applications. In this letter, the behaviors of the transverse magnetic (TM) quasi-WG modes are numerically investigated for a two-dimensional (2D) square resonator with an output waveguide connected to the midpoint of one side. The fundamental transverse and the first-order transverse modes, which have much higher Q factors than other modes in the square resonator, are considered in the simulation.

The analytical field distributions in the 2D square resonator with a side length of $4\ \mu\text{m}$ and refractive index of 3.2 are given in Figs. 1(a)–(d) for $\text{TM}_{10,12}$, $\text{TM}_{9,13}$, $\text{TM}_{11,13}$, and $\text{TM}_{10,14}$ modes^[15], respectively. $\text{TM}_{10,12}$ and $\text{TM}_{11,13}$ are the fundamental modes and $\text{TM}_{9,13}$ and $\text{TM}_{10,14}$ are the first-order modes. As shown in Fig. 1, they are standing wave and have definite parities relative to the perpendicular bisector of the square resonator. $\text{TM}_{10,12}$ and $\text{TM}_{10,14}$ modes are symmetrical to the perpendicular bisector of the square resonator with the strongest field intensity near midpoint of one side, while $\text{TM}_{9,13}$ and $\text{TM}_{11,13}$ modes are anti-symmetrical with the weakest field intensity near the midpoint of one side.

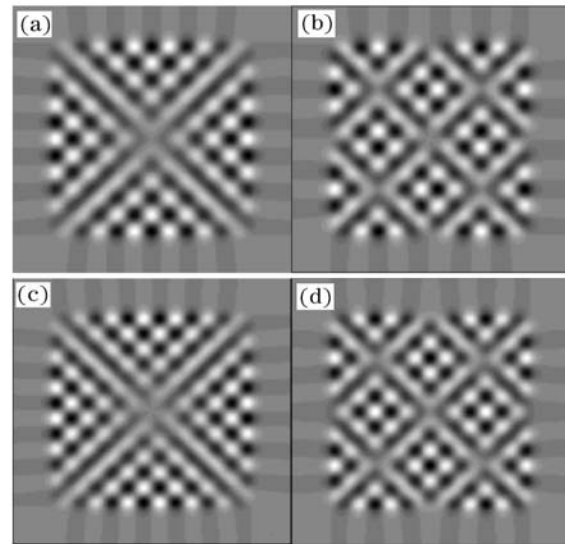


Fig. 1. Analytical field distributions of (a) $\text{TM}_{10,12}$, (b) $\text{TM}_{9,13}$, (c) $\text{TM}_{11,13}$, and (d) $\text{TM}_{10,14}$ modes in a square resonator with side length of $4\ \mu\text{m}$ and refractive index of 3.2 without an output waveguide.

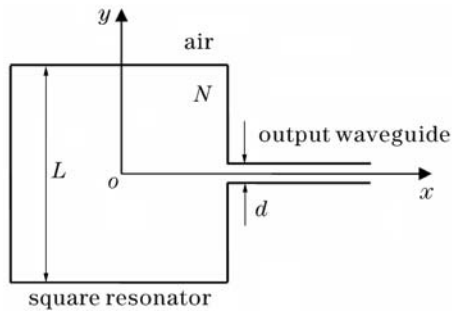


Fig. 2. Schematic diagram of the square resonator with an output waveguide.

Based on the above mode field patterns, we expect that the square resonator with an output waveguide connected to the midpoint of one side as shown in Fig. 2 can provide the directional emission output. We hope that the output waveguide can effectively guide the first-order modes but does not have a destructive effect on their Q factors. At the same time, the output waveguide can greatly decrease the Q factors of the fundamental modes and avoid their competitions with the first-order modes. In the following section, the numerical simulation analysis is used to justify the proposition by the finite-difference time-domain (FDTD) method^[18] and the Padé approximation^[19].

In the numerical calculation, we solve the Maxwell equation for a 2D square resonator with the refractive index of 3.2 surrounded by air. A uniform mesh with cell size of 20 nm and a 50-cell perfect matched layer (PML) absorbing layer are used in the FDTD simulation with the time step of the Courant limit^[18]. The following Gaussian modulating cosine function is used as the exciting sources

$$E_i(t) = \cos(2\pi ft) \exp\left[-\frac{4\pi(t-t_0)^2}{\tau^2}\right], \quad (1)$$

where f is the frequency, t is the time variable, and t_0 is the initial value.

First, we use the pulse sources covering a wide frequency range at low symmetry points of the resonator to excite all the considered TM modes, and then apply the Padé approximation method^[19] to calculate the intensity spectra from the FDTD output.

Figure 3 shows the Q factors of $TM_{10,12}$, $TM_{9,13}$, $TM_{11,13}$, and $TM_{10,14}$ modes versus the width of the

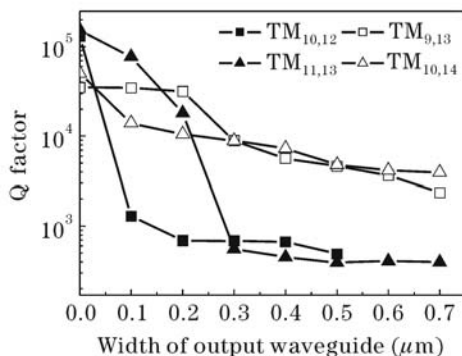


Fig. 3. Q factors of $TM_{10,12}$, $TM_{9,13}$, $TM_{11,13}$, and $TM_{10,14}$ modes are plotted as functions of the width of output waveguide for the square resonator with refractive index of 3.2 and side length of 4 μm .

output waveguide for the square resonator with side length of 4 μm . The Q factors of the fundamental modes decrease dramatically with the increase of the width of the output waveguide, while those of first-order modes change slowly relatively. When the width of the output waveguide is larger than 0.2 μm , the Q factors of the first-order modes are almost ten times as large as those of the fundamental modes. As a result, the output waveguide effectively suppresses the fundamental modes and avoids their competition with the first-order modes. In addition, the $TM_{10,14}$ can be coupled with the output waveguide because it always supports the fundamental guided modes, but $TM_{9,13}$ can be coupled into the output waveguide only when the width of the output waveguide is larger than 0.24 μm in order to support the first-order guided mode. So the Q factor of $TM_{9,13}$ almost keeps the same value as the width less than 0.2 μm . The results show that the first-order quasi-WG modes in a square resonator can be coupled into the output waveguide effectively and the Q factor can be adjusted by changing the width of the output waveguide. The square microcavity lasers can have both good mode selectivity and highly directional emission by connecting the output waveguide at the midpoint. The effect of the output waveguide on the mode wavelength is very slight. Compared with the square resonator without the output waveguide, the wavelengths of $TM_{10,12}$ and $TM_{11,13}$ in the square resonator with 0.5- μm output waveguide increase only 0.22% and 0.19%, respectively. The variations of $TM_{9,13}$ and $TM_{10,14}$ mode wavelengths almost can be neglected.

For a square resonator with the side length of 6 μm , we calculate and plot the Q factors of $TM_{16,18}$, $TM_{15,19}$, $TM_{17,19}$, and $TM_{16,20}$ modes in Fig. 4 as functions of the width of the output waveguide. $TM_{16,18}$ and $TM_{17,19}$ are the fundamental modes while $TM_{15,19}$ and $TM_{16,20}$ are the first-order modes. The results are similar to those of Fig. 3. The Q factors of the first-order modes are larger than other modes when the width of the output waveguide exceeds 0.2 μm . It indicates that the square resonator with an output waveguide has a big advantage in mode selectivity.

In order to show the high directional emission, we calculate the mode field distribution by the FDTD technique for the square resonator with 4- μm -long and 0.4- μm -wide output waveguide. The Gaussian modulating

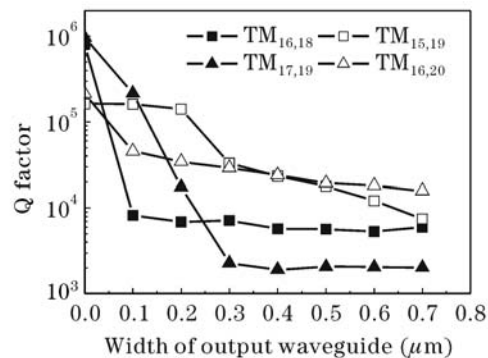


Fig. 4. Q factors of $TM_{16,18}$, $TM_{15,19}$, $TM_{17,19}$, and $TM_{16,20}$ modes are plotted as functions of the width of output waveguide for the square resonator with refractive index of 3.2 and side length of 6 μm .

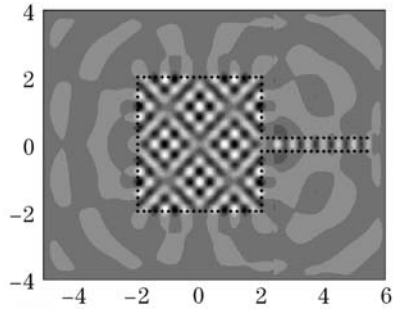


Fig. 5. Electric field distribution for $TM_{10,14}$ mode in the square resonator with side length of $4 \mu\text{m}$ and $0.4\text{-}\mu\text{m}$ -wide output waveguide. The electric field in the region of $x \geq 2.4 \mu\text{m}$ is magnified 5 times. The square resonator and the output waveguide are plotted by the dotted lines.

cosine function Eq. (1) with $f = 208.5 \text{ THz}$, $t_0 = 0.94 \text{ ps}$ and $\tau = 9/(4f)$ is used as a narrow frequency exciting source to excite only the first-order mode $TM_{10,14}$. The mode field distribution is plotted in Fig. 5, where the set of coordinates is the same as those in Fig. 2 and the electric field in the output waveguide at $x \geq 2.4 \mu\text{m}$ is magnified 5 times. It proves that $TM_{10,14}$ mode can be effectively coupled into the output waveguide. Furthermore, we also calculate the energy flux of the output waveguide through integrating the Poynting vector at the cross section of the output waveguide. Nearly 53% of the total emission energy is confined in the output waveguide. Therefore, the output power can be effectively coupled into the output waveguide and single-mode directional emission can be realized in a square resonator with an output waveguide at the midpoint of one side. Besides, we calculate the square resonator with an output waveguide which is not located at the midpoint of one side. The result shows that it has adverse effect on both Q factor and coupling efficiency.

In summary, we simulate the mode characteristics for the square resonator with an output waveguide by the FDTD technique, and prove that high output coupling efficiency and single-mode directional emission can be obtained. As a promising candidate for light sources, it might play an important role in photonic-integrated circuits.

This work was supported by the National Natural Science Foundation of China (No. 60225011) and the Major

State Basic Research Program (No. 2006CB302804). W. Zhao's e-mail address is zhaowei@semi.ac.cn.

References

1. K. J. Vahala, *Nature* **424**, 839 (2003).
2. A. F. J. Levi, R. E. Slusher, S. L. McCall, J. L. Glass, S. J. Pearton, and R. A. Logan, *Appl. Phys. Lett.* **62**, 561 (1993).
3. J. U. Nöckel, A. D. Stone, G. Chen, H. L. Grossman, and R. K. Chang, *Opt. Lett.* **21**, 1609 (1996).
4. S.-K. Kim, S.-H. Kim, G.-H. Kim, H.-G. Park, D.-J. Shin, and Y.-H. Lee, *Appl. Phys. Lett.* **84**, 861 (2004).
5. C. Gmachl, F. Capasso, E. E. Narimanov, J. U. Nöckel, A. D. Stone, J. Faise, D. L. Sivco, and A. Y. Cho, *Science* **280**, 1556 (1998).
6. J. U. Nöckel and A. D. Stone, *Nature* **385**, 45 (1997).
7. G. D. Chern, H. E. Tureci, A. D. Stone, R. K. Chang, M. Kneissl, and N. M. Johnson, *Appl. Phys. Lett.* **83**, 1710 (2003).
8. M. Leblental, J. S. Lauret, R. Hierle, and J. Zyss, *Appl. Phys. Lett.* **88**, 031108 (2006).
9. T. J. Kippenberg, S. M. Spillane, D. K. Armani, and K. J. Vahala, *Appl. Phys. Lett.* **83**, 797 (2003).
10. K. Djordjev, S.-J. Choi, S.-J. Choi, and P. D. Dapkus, *IEEE Photon. Technol. Lett.* **14**, 331 (2002).
11. S. J. Choi, K. Djordjev, S. J. Choi, and P. D. Dapkus, *IEEE Photon. Technol. Lett.* **15**, 1330 (2003).
12. I. K. Hwang and Y. H. Lee, *IEEE J. Sel. Top. Quantum Electron.* **13**, 209 (2007).
13. Y.-Z. Huang, W.-H. Guo, and Q.-M. Wang, *Appl. Phys. Lett.* **77**, 3511 (2000).
14. A. W. Poon, F. Courvoisier, and R. K. Chang, *Opt. Lett.* **26**, 632 (2001).
15. W.-H. Guo, Y.-Z. Huang, Q.-Y. Lu, and L.-J. Yu, *IEEE J. Quantum Electron.* **39**, 1563 (2003).
16. Q. Lu, X. Chen, W. Guo, L. Yu, Y. Huang, J. Wang, and Y. Luo, *Chin. Opt. Lett.* **1**, 472 (2003).
17. Y. Z. Huang, Y. H. Hu, Q. Chen, S. J. Wang, Y. Du, and Z. C. Fan, *IEEE Photon. Technol. Lett.* (to be published).
18. A. Taflove and S. C. Hargness, *Computational Electrodynamics — the Finite-Difference Time-Domain Method* (Artech House, Boston, 2000) p.133, 285.
19. W.-H. Guo, W.-J. Li, and Y.-Z. Huang, *IEEE Microwave Wireless Components Lett.* **11**, 223 (2001).